Design of High-SNR Multidimensional Constellations for Orthogonal Transmission in a Nakagami-*m* Fading Channel

HOSSEIN KHOSHNEVIS[ID], **(Student Member, IEEE), IAN MARSLAND**[ID], **(Member, IEEE),
AND HALIM YANIKOMEROGLU**[ID]**, (Fellow, IEEE)**
Department of Sytems and Computer Engineering, Carleton University, Ottawa, ON K1S 5B6, Canada
Corresponding author: Hossein Khoshnevis (khoshnevis@sce.carleton.ca)

ABSTRACT Finding the best signal constellation for different communication channels is one of the
fundamental problems in digital communication. This problem has been studied widely from different angles
and many methods have been proposed for designing good practical signal constellations. There has been a
rejuvenated interest in designing good constellations during last decade, in part due to the advent of novel
optimization techniques. Nevertheless, most of the recent work, similar to the older work in this area, aims
to optimize the constellation within a presumed structure (such as points lying on concentric rings). In this
paper, we develop a different approach: we aim to optimize constellations based on a Chernoff bound on the
probability of error in the versatile Nakagami-*m* fading channel. We derive two general bounds on the symbol
error rate and bit error rate performance of orthogonal transmission in a Nakagami-*m* fading channel for
single-input single-output and orthogonal space-time block codes and we show that a substantial improve-
ment in the error probability is achieved with the novel constellations that are optimized using these bounds.

INDEX TERMS Constellation design, Nakagami-*m* fading model, multidimensional constellations,
orthogonal space-time block codes.

I. INTRODUCTION

In wireless communication systems, high quality, capacity
and reliability are among the essential demands. One of the
key enablers for this improvement is enhanced physical layer
design by optimizing each block of the transceiver. Signal
shape design, also known as constellations design, can sub-
stantially affect the performance of communication systems.
Traditionally regular one dimensional (1D) pulse-amplitude
modulation (PAM) and 2D quadrature amplitude modula-
tion (QAM) have been widely employed in the majority of
wireless systems due to their simple decoding. However,
optimization of signal constellations provides us with better
matching between signalling and the communication chan-
nels, which may substantially improve the performance of the
system. Improving the performance of a communication sys-
tem by finding a better placement of the constellation points
has been known as the packing problem and has been studied
widely in literature by using mathematical tools such as
lattice constructions, where lattice-based constellation design

is used for finding the densest packing [1], [2]. Recently,
Beko and Dinis in [3] revisited the problem of designing
multidimensional constellations by using contemporary opti-
mization tools, whereby they minimized the sum power of all
points with a constraint on the minimum distance between
points. In spite of generating good constellations, there is
still room for improvement as this method does not consider
minimizing the number of neighbours of each constellation
point, known as the kissing number [1].

To achieve even better performance, signal constellations
can be optimized with respect to the symbol error rate (SER)
or block error rate (BLER) expressions if such expressions are
available. Since the exact error rate expressions are difficult
to derive in most cases, constellation optimization based on
either approximate expressions or bounds may prove to be a
feasible alternative. A low complexity class of upper bounds
on the performance of orthogonal transmission schemes
which assumes an arbitrary position for constellation points
can be derived by using the Chernoff bound on the pairwise

error probability (PEP) at high SNR [4], [5]. For deriving any closed-form bound on the performance in a fading channel, knowing the distribution of the fading and the number of antennas of the transceiver are essential. As a result, constellations are only designed for a specific channel.

It is well known that the bit-to-symbol mapping plays a critical role in improving the bit error rate (BER). The traditional approach in the literature for finding the BER-minimizing constellations includes two sequential steps: optimization of the constellation shape followed by optimization of the bit-to-symbol mapping [6]. However, constellation shapes optimized using a bound on BER can substantially improve the BER performance. Since the main source of bit errors at high SNR is due to the received sample falling within a decision region that is adjacent to the transmitted symbol, the SER or BLER bounds can be extended to a bound on the BER for high SNR values by considering the Hamming distance [7], [8]. As explained in Section IV, this bound can be further used for the optimization of the constellation shape.

Signal constellations in which points are mapped to more than two dimensions, hereafter called multidimensional constellations, allow for increased separation between points in comparison to the widely used 2D constellations [9]. Multidimensional constellations can be projected onto a set of orthogonal 2D signal spaces, with each projection transmitted independently. For example, a 4D symbol can be transmitted using two 2D symbols. Designing multidimensional constellations has been discussed using different techniques: in [2], [10], and [11] based on lattice construction; in [12] based on the behaviour of charged electrons in free space; and in [3] based on the optimization of non-lattice construction. However, as mentioned earlier, optimization of the bounds on the error rates of these constellations can further improve the performance.

To achieve better performance with multidimensional constellations, the constellation can be designed according to the method of transmitting different dimensions of each constellation point. One way of transmitting multidimensional constellations involves using orthogonal space-time block codes (OSTBCs). OSTBCs, as one of the main types of space-time block codes (STBCs), are used to provide full diversity with a linear complexity decoder [13], [14]. Because of their low complexity in encoding and decoding, OSTBCs have been used widely in standards [15]. However, the Alamouti scheme with two transmit antennas is the only full-rate full-diversity OSTBC; the other OSTBCs suffer from a rate loss in order to preserve their orthogonal structure.

During the last decade, there have been extensive studies on designing high-performance high-rate space-time codes, and some STBCs with higher performance and higher complexity, such as quasi-orthogonal space-time block codes (QOSTBCs) [16]–[18] and algebraic codes [19]–[32], have been introduced. One major shortcoming is that quasi-orthogonal and algebraic codes are designed for high spectral efficiencies and show rather poor performance for low to moderate spectral efficiencies. Furthermore, despite the

existence of a few studies such as [32] on designing STBCs with fewer receive antennas (N_r) than transmit antennas (N_t), most of algebraic codes are designed or work well under $N_t \leq N_r$. Therefore, they are not suitable for downlink, where the number of receive antennas in the user equipment is usually limited. Fortunately, due to the possibility of optimizing multidimensional constellations for low to moderate spectral efficiencies and for any N_t and N_r, OSTBCs with multidimensional constellations can outperform algebraic codes in their poor performance regions. Another shortcoming of most algebraic codes codes is that they are mostly designed based on the rank and determinant criteria introduced in [33] or the trace criteria [34] for a given QAM or hexagonal (HEX) constellation. However, since multidimensional constellations can be designed for SER, BLER or BER without any assumption of the constellation shape, OSTBCs with multidimensional constellations can outperform algebraic codes when the degrees of freedom of algebraic codes are not significantly higher.

Typically, an OSTBC block carries K symbols, with independent information content carried in each symbol [13]. If we employ multidimensional constellations, each 2D component of a 2K-dimensional constellation can be carried by one of the K different symbols of the OSTBC. This also can be seen as the generalization of a sphere packing problem [31]. In [5], we evaluated multidimensional constellations designed based on optimizing SER or BLER[1] bounds on the performance of OSTBCs in a Rayleigh channel. Here, we extend these bounds for the Nakagami-*m* channel. The output of the optimization problem can in general be an irregular constellation. Irregular constellations, as shown in [4] in the context of constellation rearrangement for cooperative relaying, are capable of improving the performance in comparison to regular or isometric constellations.

The main contributions of this paper are as follows:

- Derivation of bounds, with arbitrary constellation points, on the high-SNR orthogonal transmission SER and BER in Nakagami-*m* channels for the single-input single-output (SISO) antenna configuration where time is the enabler for carrying different dimensions of a constellation, and for systems with a multiple-input multiple-output (MIMO) antenna configuration where OSTBC is the enabler for carrying different dimensions of a constellation.
- Derivation of the convexity conditions of the bounds for 1D constellations.
- Optimizing 1D and multidimensional high-SNR SER-minimizing and BER-minimizing constellations based on the derived bounds for the Nakagami-*m* channel.

In particular, we demonstrate the performance advantage of the optimized 1D, 2D and multidimensional constellations in comparison to the best known constellations in the litera-

---

[1]For most parts of this paper, a block is defined as a space-time block that consists of all dimensions of a multidimensional constellation distributed in space and time. However, for the generalized scheme, introduced in Section II, a block can consist of several multidimensional constellations.

ture, and we show how much gain is achieved by adapting the constellation in the Nakagami-*m* channel based on the channel parameter *m*. In addition, we show that the optimization problems for the case of 1D constellations are convex under a specific condition and we explain a set of methods to solve the convex and non-convex optimization problems efficiently. Furthermore, we show that the space-time constellations optimized using the proposed bounds outperform the best known space-time constellations in a Nakagami-*m* channel.

The rest of the paper is organized as follows: The system model is described in Section II, union bounds on the probability of error are derived in Section III, the optimization criteria and algorithms are provided in Section IV, simulation results are reported in Section V, and the conclusions are presented in Section VI.

Throughout this paper, to uniquely identify the constellations, the format *M*-*N*D is used where *M* is the number of points and *N* is the number of dimensions of a constellation; to show the 2D QAM and HEX constellations, the format *M*-QAM or *M*-HEX is employed. For example, 16-2D represents a 2D constellation with 16 points.

II. SYSTEM MODEL

The system considered in this paper consists of multiple transmit antennas that use STBCs. The data is divided into groups of *d* bits and accordingly mapped to symbols of different 2D constellations which are projections of a $2K$-dimensional constellation with a modulation order of 2^d. The system is equipped with N_t and N_r antennas at the transmitter and receiver, respectively, and each space-time code block consists of *L* time slots. Each symbol is transmitted through a block fading channel denoted by the $N_t \times N_r$ matrix **H**, with elements $h_{ij} = \alpha_{ij}e^{j\phi_{ij}}$ where α_{ij} has a Nakagami-*m* distribution. The system can be described as

$$\mathbf{R} = \mathbf{GH} + \mathbf{W}, \tag{1}$$

where **R** is the $L \times N_r$ received matrix, **G** is the $L \times N_t$ transmitted STBC block, and **W** represents the additive white Gaussian noise (AWGN) where each element of **W** is an independent and identically distributed (iid) complex Gaussian with zero-mean and variance $N_0/2$ per dimension. The average power of the transmitted matrix **G** is set to one. The Nakagami-*m* fading distribution is used as the general model for fading statistics because it provides a good match to a wide set of empirical measurements. The corresponding SNR distribution can be expressed as

$$f_{m,\bar{\gamma}_{ij}}\left(\gamma_{ij}\right) = \frac{m^m}{\bar{\gamma}_{ij}^m \Gamma(m)} \gamma^{m-1} e^{-m\gamma_{ij}/\bar{\gamma}_{ij}}, \tag{2}$$

where $\Gamma\left(\cdot\right)$ is the Gamma function, $\bar{\gamma}_{ij} = E[\alpha_{ij}^2]/N_0$ is the average SNR of each path and *m* is the shape parameter which is fixed for all paths. For simplicity, we set $E[\alpha_{ij}^2] = 1$. The Rayleigh channel, as a special case of the Nakagami-*m* model, can be obtained by setting $m = 1$. By denoting c_i^l as the space-time code symbol transmitted in time slot *l* from antenna *i*, the general maximum likelihood (ML)

decoding rule in the receiver for the transmission of codeword $\mathbf{c} = c_1^1 c_2^1 \ldots c_{N_t}^1 \ldots c_1^L c_2^L \ldots c_{N_t}^L$ in an $L \times N_t$ space-time block using perfect channel state information can be expressed as the minimization of the following metric over all constellation points:

$$\sum_{l=1}^{L} \sum_{j=1}^{N_r} \left| r_j^l - \sum_{i=1}^{N_t} h_{ij} c_i^l \right|^2. \tag{3}$$

where r_j^l is the received sample on the jth antenna in time slot *l*. For orthogonal transmission using the space and time resources, different antenna configurations can be used such as SISO and MIMO. In a SISO configuration, the consecutive time slots may be employed as the time resources, while in MIMO, STBCs can be employed to use both space and time resources for transmission of different dimensions of multidimensional constellations.

OSTBCs are general structures that can be employed for carrying data orthogonally over fading channels. Their simplest form, proposed by Alamouti [14] for two transmit antennas, can be written as

$$\mathbf{G}_0 = \begin{bmatrix} s_1 & s_2 \\ -s_2^* & s_1^* \end{bmatrix}. \tag{4}$$

In Code $\mathbf{G}_0$, data are mapped separately to each constellation point and carried by symbols s_1 and s_2, both of which are independent elements of a 2D constellation, $\mathcal{S}_2$. As described in Section I, to transmit multidimensional constellations using OSTBCs, their 2D components are distributed on OSTBC symbols. By considering s_1 and s_2 used in $\mathbf{G}_0$ as carriers of the 2D components of a multidimensional constellation, Alamouti's scheme can be rewritten as

$$\mathbf{G}_1 = \begin{bmatrix} s^{(1)} & s^{(2)} \\ -s^{(2)*} & s^{(1)*} \end{bmatrix}, \tag{5}$$

where $s^{(k)}$ is the kth 2D component for transmission of a multidimensional symbol $\mathbf{s} = [s^{(1)}, s^{(2)}, \ldots, s^{(K)}]$ with $\mathbf{s} \in \mathcal{S}_{2K}$, a $2K$-dimensional constellation. In $\mathbf{G}_1$, data are mapped to two 2D subpoints of a 4D point and the subpoints are carried by $s^{(1)}$ and $s^{(2)}$. As an example, to provide a spectral efficiency of 2 bits per channel-use (bpcu), a 4-QAM constellation should be used for s_1 and s_2 in $\mathbf{G}_0$, whereas a 16-4D constellation should be used for $\mathbf{s} = [s^{(1)}, s^{(2)}]$ in $\mathbf{G}_1$.

For the case of four-antenna transmission, the well known OSTBC presented in [35] can be rewritten for multidimensional constellations as

$$\mathbf{G}_2 = \begin{bmatrix} s^{(1)} & s^{(2)} & s^{(3)} & 0 \\ -s^{(2)*} & s^{(1)*} & 0 & s^{(3)} \\ s^{(3)*} & 0 & -s^{(1)*} & s^{(2)} \\ 0 & s^{(3)*} & -s^{(2)*} & -s^{(1)} \end{bmatrix}, \tag{6}$$

and, by dropping the last column of $\mathbf{G}_2$, the corresponding scheme for a three-antenna transmission of a 6D constellation

can be written as

$$\mathbf{G}_3 = \begin{bmatrix} s^{(1)} & s^{(2)} & s^{(3)} \\ -s^{(2)*} & s^{(1)*} & 0 \\ s^{(3)*} & 0 & -s^{(1)*} \\ 0 & s^{(3)*} & -s^{(2)*} \end{bmatrix}. \qquad (7)$$

By using the orthogonal structure of OSTBCs, a simplified ML decoder can detect s_k according to

$$\hat{s}_k = \underset{\forall s \in \mathcal{S}_2}{\operatorname{argmin}} \left| P_k - \left(\sum_{i,j} \alpha_{ij}^2 \right) s \right|^2, \qquad (8)$$

where

$$P_k = \sum_{j=1}^{N_r} \sum_{l=1}^{L} \sum_{i=1}^{N_t} F_{i,k}^l (r_j^l h_{ij}^*). \qquad (9)$$

In (9), $k = 1, 2, \ldots, K$ shows the index of the different symbols carried by one OSTBC block and $F_{i,k}^l(z)$ can be evaluated as

$$F_{i,k}^l(z) = \begin{cases} z, & \text{if } c_i^l = s_k, \\ z^*, & \text{if } c_i^l = s_k^*, \\ -z, & \text{if } c_i^l = -s_k, \\ -z^*, & \text{if } c_i^l = -s_k^*, \\ 0, & \text{otherwise.} \end{cases} \qquad (10)$$

This simplified decoder can be used for decoding the multidimensional constellations by changing (8) into a summation of decoding of different 2D components of the multidimensional constellations, expressed as

$$\hat{\mathbf{s}} = \underset{\forall \mathbf{s} \in \mathcal{S}_{2K}}{\operatorname{argmin}} \sum_{k=1}^{K} \left| P_k - \left(\sum_{ij} \alpha_{ij}^2 \right) s^{(k)} \right|^2. \qquad (11)$$

Note that the term P_k should be computed only once for each k, as this substantially decreases the complexity of decoding in comparison to the high-performance complex codes such as the perfect codes [26], [27] in which (3) may need to be computed for all points of a constellation.

Up to now, only transmission of one multidimensional symbol per codeword has been discussed. However, by considering the independence of 2D symbols in the OSTBC structure, a codeword can be split to carry symbols of multiple independent multidimensional constellations with different numbers of dimensions. As an example, $\mathbf{G}_3$ can be split to carry two 2D components of one 4D constellation and one 2D constellation; the new codeword can be written as

$$\mathbf{G}_4 = \begin{bmatrix} s_1^{(1)} & s_1^{(2)} & s_2^{(1)} \\ -s_1^{(2)*} & s_1^{(1)*} & 0 \\ s_1^{(1)*} & 0 & -s_1^{(1)*} \\ 0 & s_2^{(1)} & -s_1^{(2)*} \end{bmatrix}. \qquad (12)$$

This generalized scheme can provide a performance-complexity trade-off in comparison to the base scheme

described above where we used all independent 2D symbols of an OSTBC to carry dependent 2D symbols of a multidimensional constellation. In this scheme, since all 2D resources are not used, the number of dimensions of the multidimensional constellation decreases, which reduces the complexity of each search in ML decoding. To maintain the same spectral efficiency, the number of points can also be decreased, and, therefore, the number of searches in ML decoding decreases as well. Even though the complexity reduction results in performance degradation in comparison to the base scheme, the scheme still preserves considerable gain, especially when the OSTBC has a large size. As an example for achieving the spectral efficiency of 1.5 bpcu, $\mathbf{G}_3$ can be used with a 64-6D constellation, whereas $\mathbf{G}_4$ can be used with a 16-4D constellation for $[s_1^{(1)}, s_1^{(2)}]$ and a QPSK constellation for $s_2^{(1)}$.

III. UPPER BOUNDS ON THE PERFORMANCE

In this section, we derive three general bounds on the performance of an OSTBC with multidimensional constellations. 1D and 2D constellations and SISO antenna configuration are special cases of this bound. Although certain bounds on performance of OSTBCs exists in the literature [36], a specific bound based on the position of points is necessary to optimize the constellation. We start with a bound on the SER. Due to the orthogonal structure of the OSTBC, its PEP is given by [35]

$$P(\mathbf{s} \to \hat{\mathbf{s}} \mid \mathbf{H}) = $$
$$Q \left(\sqrt{ \left(\frac{\sum_{j=1}^{N_r} \sum_{i=1}^{N_t} \alpha_{ij}^2}{2N_0} \right) \sum_{k=1}^{K} \left| s^{(k)} - \hat{s}^{(k)} \right|^2 } \right), \quad (13)$$

where $Q(\cdot)$ is the Gaussian tail function. By using the Chernoff bound on (13), a union bound on the SER of OSTBCs can be written as

$$P_s \leq \frac{1}{2^d} \sum_{v=1}^{2^d} \sum_{\substack{v'=1 \\ v' \neq v}}^{2^d} \frac{(4)^{mN_tN_r}}{\prod_{j=1}^{N_r} \prod_{i=1}^{N_t} \left(\frac{\bar{\gamma}_{ij}}{m} \sum_{k=1}^{K} \left| s_v^{(k)} - s_{v'}^{(k)} \right|^2 + 4 \right)^m}, \qquad (14)$$

The derivation of (14) is presented in Appendix A.1.

Proposition 1: In the case of 1D constellations, the union bound in (14) is a convex function on the convex set

$$\left\{ -(1 - e_{vv'})\mathbb{L} + e_{vv'}x < s_v - s_{v'} < -(1 - e_{vv'})x + e_{vv'}\mathbb{L}, \right.$$
$$\left. \forall e_{vv'} \in \{0, 1\}, \forall v, v' \in \{1, \ldots, 2^d\} \right\}, \qquad (15)$$

where $\mathbb{L}$ is a large positive number, $e_{vv'}$ is a binary variable and x is given by

$$x = \frac{2}{\sqrt{\bar{\gamma}(2 + \frac{1}{mN_tN_r})}}, \qquad (16)$$

where $\bar{\gamma}$ is the total average SNR for each received matrix $\mathbf{G}$.

Proof: In Appendix B.1. ∎

In (16), when $m \to \infty$ or $N_t N_r >> 1$, x tends to $\sqrt{2}/\bar{\gamma}$ and in the limit of high SNR, x tends to zero. The union bound in (14) can be upper bounded as

$$P_s \leq \frac{1}{2^d} \sum_{v=1}^{2^d} \sum_{\substack{v'=1 \\ v' \neq v}}^{2^d} \frac{(4m)^{mN_t N_r}}{\mu \left(\sum_{k=1}^{K} \left| s_v^{(k)} - s_{v'}^{(k)} \right|^2 \right)^{mN_t N_r}}, \quad (17)$$

where μ is defined as

$$\mu := \prod_{j=1}^{N_r} \prod_{i=1}^{N_t} \bar{\gamma}_{ij}. \quad (18)$$

The derivation of (17) is presented in Appendix A.2.

Proposition 2: In the case of 1D constellations, the union bound in (17) is a convex function on the convex set

$$\left\{ 0 < s_{v'} - s_v < \mathbb{L}, \forall v \in \{1, \ldots, 2^d\}, v' \in \{v+1, \ldots, 2^d\} \right\}. \quad (19)$$

Proof: In Appendix B.2. ∎

For the case of the Rayleigh channel, which corresponds to $m = 1$ in the Nakagami-m model, (17) can be simplified to

$$P_s \leq \frac{1}{2^d} \sum_{v=1}^{2^d} \sum_{\substack{v'=1 \\ v' \neq v}}^{2^d} \frac{4^{N_t N_r}}{\mu \left(\sum_{k=1}^{K} \left| s_v^{(k)} - s_{v'}^{(k)} \right|^2 \right)^{N_t N_r}}. \quad (20)$$

For the AWGN channel, which corresponds to the limiting case in Nakagami-m model with $m \to \infty$, the bound is given by

$$P_s \leq \frac{1}{2^d} \sum_{v=1}^{2^d} \sum_{\substack{v'=1 \\ v' \neq v}}^{2^d} \exp\left(-\frac{N_t N_r}{4N_0} \sum_{k=1}^{K} \left| s_v^{(k)} - s_{v'}^{(k)} \right|^2 \right). \quad (21)$$

A simple proof for (21) is presented in Appendix A.3.

If, in each space-time block of the scheme, only one symbol from the multidimensional constellation is transmitted, the SER and BLER of the STBC block become identical. Therefore, the above bound can be used for finding the locally optimum constellations for minimizing the BLER of a space-time block. For the generalized scheme, the SER bound is used to optimize different-sized independent multidimensional constellations used with the scheme, even though this is no longer an appropriate bound on the BLER.

By considering the Hamming distance $\mathcal{H}(v, v')$ between each pair of constellation points, the corresponding bound on the BER can be written as

$$P_b \leq \frac{1}{d2^d} \sum_{v=1}^{2^d} \sum_{\substack{v'=1 \\ v' \neq v}}^{2^d} \frac{\mathcal{H}(v, v')(4m)^{mN_t N_r}}{\mu \left(\sum_{k=1}^{K} \left| s_v^{(k)} - s_{v'}^{(k)} \right|^2 \right)^{mN_t N_r}}. \quad (22)$$

For 1D constellations, labels of the constellation points are found by considering the weights $\mathcal{H}(s, \hat{s})$. Hence, both $s_v > s_{v'}$ and $s_v < s_{v'}$ may happen. If we consider all possibilities for the sign of pairwise differences, $2^{(2^d-1)!}$ different

subproblems should be solved. Therefore, the optimization procedure is not possible in polynomial time. In addition, solving all subproblems limits the convexity to the case of $mN_t N_r \in \mathcal{N}$. However, for a specific labelling, e.g. Gray mapping, only one subproblem should be solved. Here, we show that under a specific bit-to-symbol mapping, (22) is convex.

Proposition 3: In the case of 1D constellations, for a given bit-to-symbol mapping, the union bound in (22) is a convex function on the convex set defined in (19).

Proof: It is shown in Appendix B.2 that for 1D constellations (17) is a convex function on the convex set defined in (19). In the proof, we assumed $s_1 \leq s_2 \leq \ldots \leq s_{2^d}$. To keep this condition, the weights $\hat{\mathcal{H}}(v, v') = \mathcal{H}(a_v, a_{v'})$ should be used instead of $\mathcal{H}(v, v')$ in (22), where $\mathbf{a}$ is the vector of indices of a given mapping. $\hat{\mathcal{H}}(v, v')$ is always a non-negative integer and the non-negative weighted sum of convex functions is also a convex function [37]. Hence, (22) is convex on (19) for a given bit-to-symbol mapping. ∎

One of the important factors in deriving bounds for the optimization of constellations is considering their complexity. For example, well-known union bounds on the performance of constellations in the AWGN channel based on Q(·) function in [38] are quite difficult to optimize for medium-to-large constellations since each evaluation of Q(·) takes a relatively long time in comparison to the simplified bounds presented in (17), (20), (21), and (22). Furthermore, in many cases, optimization based on more complex bounds results in very little improvement. Therefore, throughout this paper, we only optimize (17) and (22) to find SER-minimizing and BER-minimizing 1D, 2D and multidimensional constellations.

IV. OPTIMIZATION CRITERIA AND ALGORITHMS

In this section, the optimization problems, optimization procedure and the choice of the method, are discussed. The labelling search algorithm as the second method of finding BER improving constellations is explained. Furthermore, samples of optimized constellations are shown.

A. OPTIMIZATION PROBLEMS

For finding optimized constellations, the union bound given in (17) on the BLER is minimized. To improve the performance by employing the shaping instead of increasing the power, the only constraint used in the optimization of multidimensional constellations is that the average power of the constellation points is limited to one. The optimization problem for minimizing BLER is to find $s_v^{(k)}$ for all $k \in \{1, \ldots, K\}$ and $v \in \{1, \ldots, 2^d\}$ that will

$$\text{minimize} \sum_{v=1}^{2^d} \sum_{v'=v+1}^{2^d} \frac{C}{\left(\sum_{k=1}^{K} \left| s_v^{(k)} - s_{v'}^{(k)} \right|^2 \right)^{mN_t N_r}},$$

$$\text{subject to} \frac{1}{2^d K} \sum_{v=1}^{2^d} \sum_{k=1}^{K} \left| s_v^{(k)} \right|^2 \leq 1, \quad (23)$$

where $C = 2(4m)^{mN_tN_r}/(2^d\mu)$, which is a constant and does not affect the optimization. In (23), v' is started from $v+1$, since $|s_v^{(k)} - s_{v'}^{(k)}|$ and $|s_{v'}^{(k)} - s_v^{(k)}|$ result in an equal PEP. Note that (23) does not depend on μ and therefore the output of the optimization is an SNR-independent constellation. For the case of the BER optimization, the problem is written as

$$\text{minimize} \sum_{v=1}^{2^d} \sum_{v'=v+1}^{2^d} \frac{\mathcal{H}(v,v')C'}{\left(\sum_{k=1}^{K} \left|s_v^{(k)} - s_{v'}^{(k)}\right|^2\right)^{mN_tN_r}},$$

$$\text{subject to} \frac{1}{2^d K} \sum_{v=1}^{2^d} \sum_{k=1}^{K} \left|s_v^{(k)}\right|^2 \leq 1, \quad (24)$$

where $C' = 2(4m)^{mN_tN_r}/(d2^d\mu)$. Due to convexity of the problem for 1D constellations, the following convex programs are used to optimize 1D constellations by minimizing the SER and the BER, respectively:

$$\text{Minimize} \sum_{v=1}^{2^d} \sum_{v'=v+1}^{2^d} \frac{C}{(s_v - s_{v'})^{2mN_tN_r}},$$

$$\text{subject to} \frac{1}{2^d} \sum_{v=1}^{2^d} |s_v|^2 \leq 1,$$

$$s_{v'} - s_v \leq \mathbb{L}, s_{v'} - s_v \geq 0,$$

$$\forall v \in \{1, \dots, 2^d\}, v' \in \{v+1, \dots, 2^d\}. \quad (25)$$

$$\text{Minimize} \sum_{v=1}^{2^d} \sum_{v'=v+1}^{2^d} \frac{\hat{\mathcal{H}}(v,v')C'}{(s_v - s_{v'})^{2mN_tN_r}},$$

$$\text{subject to} \frac{1}{2^d} \sum_{v=1}^{2^d} |s_v|^2 \leq 1,$$

$$s_{v'} - s_v \leq \mathbb{L}, s_{v'} - s_v \geq 0,$$

$$\forall v \in \{1, \dots, 2^d\}, v' \in \{v+1, \dots, 2^d\}. \quad (26)$$

In (25) and (26), due to the normalization of the total constellation power to one, the distance of points cannot be greater than two. As such, we set $\mathbb{L} = 2$. Note that the equalities in constraints are not activated. Otherwise, the objective function tends to infinity.

B. OPTIMIZATION PROCEDURE AND THE CHOICE OF THE METHOD

The constellations optimized in this paper do not need to be updated. Thus, only offline optimization is discussed in this section. For the nonlinear programs (NLPs) in (23) and (24), two optimization methods, including the interior-point method (IPM) and the sequential quadratic programming method (SQPM), were employed. These two classes of methods are typically used for solving constrained optimization problems. IPM works based on the iterative moving in the interior of the feasible set, determined using the constraints, and decreasing a multiplier until a perturbed Karush–Kuhn–Tucker (KKT) conditions tends to the original KKT. IPM initially walks far from the boundary of the feasible set and

iteratively gets closer to the boundary. In each iteration of the SQPM, a quadratic program, which is generated by the quadratic approximation of the objective function, is solved. At each step, the Jacobian and the Hessian are approximated and a step length is determined using a line search in the direction of the minima. Each iteration in IPM typically is more complex than SQPM but fewer iterations are needed to achieve a good solution. For a detailed description of IPM see [39], [40], and for SQPM see [6], [40] and references therein. In the both cases, the step size decrease as the solver goes closer to a local optima. Thus, the minimum step size is used as the stopping criteria. As the size of the constellation, and consequently the number of variables, increases, we need to increase the maximum number of iterations. As m, N_t, or N_r increases, the complexity of computation of the Jacobian and Hessian and estimation of the quadratic program increases and the optimization slows down. For all methods, the vector of complex symbols is transferred to the double-size vector of real variables.

For both small and large constellations, e.g., 16-2D and 256-4D, both IPM and SQPM converge to a locally optimum solution with a very similar objective function value. However, in all cases SQPM converges to the best final value faster. In contrast, IPM finds a solution within ±1% of the final solution faster. As an example, for optimization of a 256-4D SER-minimizing constellation, IPM finds a good solution in the feasibility region in around 51000 steps. This takes around 200 seconds using Matlab on a computer with 24 GB RAM and a 3.40 GHz i7-3770 CPU. In comparison, SQPM finds the same solution in around 160000 steps, which takes around 300 seconds, by setting $m = 1$, $N_t = 1$ and $N_r = 1$. Although further optimization is not effective on the performance of the system, SQPM and IPM converge to the best achievable solution in around 410000 and 670000 steps, corresponding to around 700 and 2200 seconds, respectively. In fact, since IPM can move far from the boundary of the feasible set, it converges faster to a good solution. In the long run, since the computation of each step in SQPM is cheaper, SQPM can move deeper in the feasible set during a limited time and generates slightly better results. Nevertheless, for large constellations, IPM finds a good solution faster than SQPM. Therefore, it is used as the preferred optimization method in this paper.

To improve the results, we restart the solver from a slightly perturbed starting point sequentially to find several locally minimum solutions and we choose the best of these. For generating new starting points, small perturbation coefficients from $\mathcal{CN}(0, 0.2)$ are randomly generated and added to the initial starting point. Then the new starting point total power is normalized to satisfy the power constraint in (23) and (24).

In addition to IPM and SQPM, we also examined simulated annealing (SA) in [41] and genetic algorithm (GA) as two well known methods of global optimization. For the case of an SA algorithm, although improvement in bound value is observable, it converges very slowly and the results are worse than the solution found using IPM and SQPM. For GA,

the results were even worse as it does not find any useful solution. Indeed, due to the continues nature of the feasible set, evolutionary algorithms cannot find good solutions.

The convex problems in (25) and (26) can be modelled and solved using cvx. Due to energy efficiency, optimum constellations for coherent systems have zero mean. It has been shown that they are typically symmetric around zero [44]. Therefore, as a good solution, we can optimize the constellation for the positive points alone, i.e., $s_{2(d-1)}, \ldots, s_{2^d}$. Therefore, we only have $2^{(d-1)}$ free variables to optimize. Thus, for optimization of a 1D constellation with $d = 6$, only 32 variables should be optimized. For the case of the BER-minimizing constellation, we set the bit-to-symbol mapping to Gray. Gray mapping is optimal at high SNR for regular constellations in the AWGN channel [44]. Here, we assume it remains good in the Nakagami-*m* channel. For the sake of comparison, we also used IPM to solve the equivalent 1D problems in (23) and (24) to find locally optimal solutions. The result shows that the convex optimization of a 16-1D constellation, can provide up to 0.2 dB better results than non-convex optimization.

To initiate the solver for optimizing based on the SER or BLER with a good starting point, all constellations are initially selected from the Cartesian product of PAM constellations known as cubic constellations [10]. For example, the rectangular QAM constellations are used as the initial point for optimization of 2D constellations. To initiate the optimization for minimizing the BER, the Cartesian product of Gray-mapped PAM constellations is employed.

For optimization in the AWGN channel, a value of $m = 10$ is used in optimization problems (23) and (24) instead of a very large m, since large values of m slows down the optimization procedure and Nakagami-*m* fading with $m = 10$ is close enough to the AWGN channel. Alternatively, the bound (21) can be used for the optimization of constellations in the AWGN channel. However, the result of optimization with this bound does not show good performance since the SNR knowledge is necessary for finding good constellations.

C. TWO-STEP OPTIMIZATION OF BER-MINIMIZING CONSTELLATIONS

Traditionally, to optimize the constellation for minimizing the BER, a two-step process is used. First an optimum constellation is found based on the shaping metric; and second, the bit-to-symbol mapping is optimized by using an appropriate metric [6]. Therefore, two independent steps are needed to find an optimum constellation for minimizing the BER. For example, in our case, the bound (17) on the SER is used to find a constellation with a good shape and then by using an appropriate algorithm, such as the binary switching algorithm in [42], [43], and [45], the best bit-to-symbol mapping is found. To find the bit-to-symbol mapping, we modify the binary switching algorithm to adapt it to our problem. The labelling algorithm can be described as Algorithm 1, where

---

Algorithm 1 Binary Switching Algorithm

Input: SER optimized constellation points $\mathbf{s}$
Output: A locally optimum bit to symbol mapping $\mathbf{z}^*$ for $\mathbf{s}$
   Procedures used in the algorithm:
   ●*SORT_INDICES(): Sorts out and returns a vector of indices of constellation points in decreasing order of cost function C.*
   ●*SWITCH_INDEX(i,j): Switch the index of ith and j^{th} constellation points in $\mathbf{s}$ and returns the new index vector.*
   ●*UPDATE_COST(): Calculates and returns the cost of each point based on (27) and the total cost based on (28).*
   Variables:
   δ: Vector of sorted costs of constellation points.
   $\mathbf{z},\mathbf{z}'$: Vectors of indices of constellation points.
   D,Δ: Total cost value.
   I_{Max}: Number of iterations.
   Initialisation:
1: Randomly choose an index vector $\mathbf{z}$ for constellation points $\mathbf{s}$ and sort them out based on the random index vector.
   The body of Algorithm:
2: $\mathbf{z}^*=\mathbf{z}$
3: **for** $I = 1$ to I_{Max} **do**
4:     $[\Delta,\delta]$=UPDATE_COST($\mathbf{s}(\mathbf{z}^*)$)
5:     $\mathbf{z}$=SORT_INDICES($\delta,\mathbf{z}^*$)
6:     v=1
7:     Indicator=0
8:     IterationFinishFlag=0
9:     **while** (IterationFinishFlag==0) **do**
10:         **for** $v' = 1$ to 2^d **do**
11:             **if** ($\mathbf{z}(v) \neq v'$) **then**
12:                 $\mathbf{z}'$=SWITCH_INDEX($\mathbf{z}(v),v'$)
13:                 D=UPDATE_COST($\mathbf{s}(\mathbf{z}')$)
14:                 **if** ($D < \Delta$) **then**
15:                     $\Delta = D$
16:                     $\mathbf{z}^* = \mathbf{z}'$
17:                     Indicator=1
18:                 **end if**
19:             **end if**
20:             SWITCH_INDEX($v',\mathbf{z}(v)$)
21:         **end for**
22:         **if** (Indicator==1) $\|$ ($v == 2^d$) **then**
23:             IterationFinishFlag=1
24:         **else if** Indicator==0 **then**
25:             v=v+1
26:         **end if**
27:     **end while**
28: **end for**
29: **return** $\mathbf{z}^*$

$c(v)$ is the cost of each symbol and can be calculated as

$$c(v) = \sum_{\substack{v'=1 \\ v' \neq v}}^{2^d} \frac{H(v,v')C'}{\left(\sum_{k=1}^{K} \left|s_v^{(k)} - s_{v'}^{(k)}\right|^2\right)^{mN_tN_r}}. \qquad (27)$$

The total cost can be calculated as the sum of the cost function of each symbol and can be expressed as

$$c_{tot} = \sum_{v=1}^{2^d} c(v). \qquad (28)$$

The binary switching algorithm is initialized by a random index vector. The individual cost of points for each index v in constellation and the total cost of the bit-to-symbol

mapping is computed using the *UPDATE_COST*() function based on (27) and (28), respectively. The individual pairwise cost of points for each point *v* are first sorted out using the *SORT_INDICES*() function in decreasing order. Then, the algorithm swaps the index of the point with the highest individual cost with all other points using *SWITCH_INDEX*() to find a mapping with a lower total cost. Indeed, it is assumed that the highest individual cost should be suppressed first. In case no improvement is achieved by switching the indices, the same procedure is repeated for the rest of the sorted indices in **z** in decreasing order. If a better bit-to-symbol mapping is found, the Algorithm 1 starts the next iteration. In case of no improvement after checking all indices in **z**, the algorithm is halted.

By switching the indices, any index vector can be achieved from any other index vector [42]. Therefore, the globally optimal solution is not out of the achievable range of the solutions, although it is hard to achieve. Here, we choose to start the new iteration after finding an improved bit-to-symbol mapping instead of checking all elements of **z** to avoid the greediness. We also examined the case of choosing the best mapping by checking all sorted elements of **z** in each iteration which resulted in worse mappings for many constellations due to being more greedy.

To achieve a better result in limited time, Algorithm 1 can be excited many times with different initial points specified by different random vectors, **z**. Here, we choose to have 10000 different initial points since more than that rarely improves the quality of optimization for small to medium-size constellations.

In Section V, we compare the result of the two-steps optimization method with the constellations achieved using the bound (22) on the BER which corresponds to the joint optimization of constellation shaping and bit-to-symbol mapping. We show that the constellations achieved using the optimization of (22) outperform the constellations achieved using the two-step method.
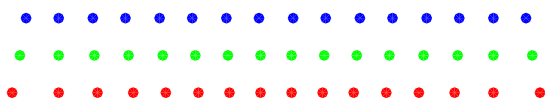

FIGURE 1. Comparison of 1D 16-PAM SER optimized constellations for the AWGN channel (top, in blue), the Nakagami-*m* channel with $m = 3$ (middle, in green), and the Rayleigh channel, i.e., Nakagami-*m* with $m = 1$ (bottom, in red).

D. SAMPLES OF OPTIMIZED CONSTELLATIONS
By optimizing problems of Section IV-A, constellations with improved performance in comparison to the PAM and QAM constellations are achieved. Fig. 1 shows samples of 16-1D constellations optimized by solving the problem (23) for the Nakagami-*m* fading channel. We observe that while for the AWGN channel, approximately equidistant PAM constellations are known to outperform other constellations, the optimal shape is quite different for other cases including Nakagami-*m* with $m = 3$ and Rayleigh fading.

The best known 2D constellations in high SNR for minimizing the SER are Voronoi constellations, where signal points are positioned approximately on a hexagonal grid which we refer to as the HEX constellations [46]–[48] or penny packing [49]. Fig. 2(a) shows a sample of 16-2D constellations optimized by solving the problem (23). Interestingly, the optimized constellation for the AWGN channel is HEX-like while the one for the Rayleigh channel is on two polygons (one inside of the other) with a zero amplitude point in the middle. Fig. 2(b) shows the samples of the optimized 2D constellations for minimizing the BER by solving the problem (24). Interestingly, for the AWGN channel, the optimized constellation is a HEX-like one, while for the Rayleigh channel it is only slightly different from a 16-QAM constellation.

QAM constellations with order 2^d, $d \in 3, 5, 7, \ldots 2n + 1$, are not energy efficient. However, by solving (23), energy efficient alternatives can be generated. Fig. 2(c) and Fig. 2(d) illustrates the 8-2D constellations optimized for the SER and BER of the AWGN and Rayleigh fading channels, respectively.

The two 2D projections of a sample optimized 16-4D constellation is plotted in Fig. 3. In this figure, each 2D constellation point represents two dimensions of a 4D constellation point, and points with the same label are indicated with the same marker and colour. This figure shows that constellation points generated by solving (23) can be irregularly placed anywhere in the signal space.

V. PERFORMANCE EVALUATION AND DISCUSSION
In this section, we evaluate the performance of the constellations optimized in Section IV in comparison to the best-known constellations in the literature. The channel is modelled as experiencing uncorrelated Nakagami-*m* fading with AWGN. The results of SISO and MIMO antenna configurations are discussed in the first and the second parts of this section, respectively.

A. RESULTS FOR THE SISO CONFIGURATION
In this section, the performance of constellations optimized for the SISO configuration are evaluated. For comparison, constellations were also optimized by using a bound on the SER of the SISO AWGN channel in [47], [50], and [51]. The corresponding optimization problem can be written as

$$\text{minimize} \quad \frac{1}{2^d \sqrt{2\pi}} \sum_{v=1}^{2^d} \sum_{\substack{v'=1 \\ v' \neq v}}^{2^d} \frac{\exp\left(-\frac{1}{4N_0} |s_v - s_{v'}|^2\right)}{\frac{1}{\sqrt{2N_0}} |s_v - s_{v'}|^2},$$

$$\text{subject to} \quad \frac{1}{2^d} \sum_{v=1}^{2^d} |s_v|^2 \leq 1. \tag{29}$$

For the optimization of 2D constellations based on (29), the SNR is set to 20 dB (the SNR value is required for this optimization and we found the best results at the mentioned value).
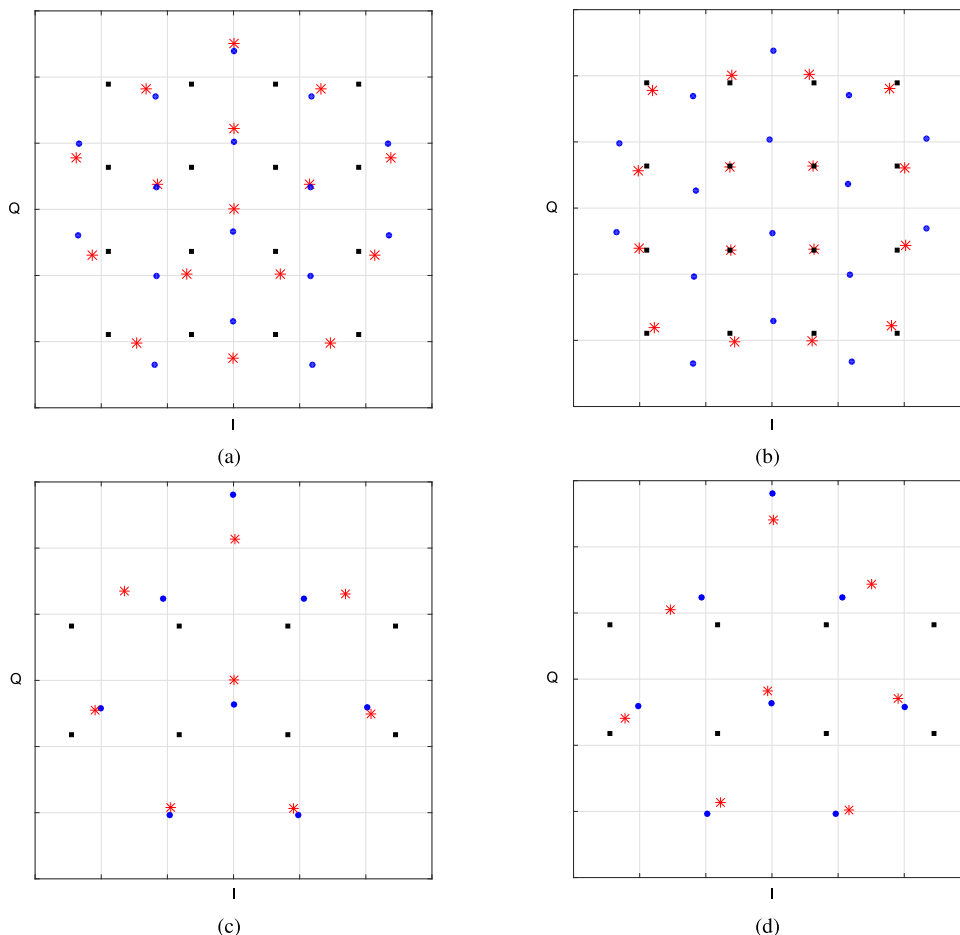
FIGURE 2. Comparison of a) 16-QAM and 16-2D SER optimized constellations, b) 16-QAM and 16-2D BER optimized constellations, c) 8-QAM and 16-2D SER optimized constellations and d) 8-QAM and 16-2D BER optimized constellations. The QAM constellations are shown with black squares and the optimized constellations for AWGN and the Rayleigh fading channel are shown with blue circles and red asterisks, respectively.
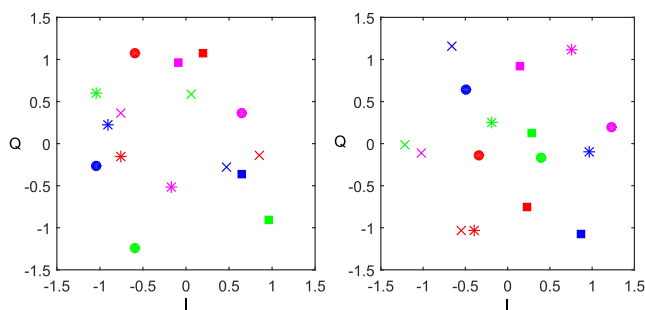

FIGURE 3. Sample of the optimized 16-4D constellation used for the scheme G_1.

In Fig. 4, the BLER of 64-1D constellations has been evaluated in the Nakagami-m channel with different m values and for the spectral efficiency of 6 bpcu. In each case, the performance of the optimized constellation for the corresponding m-factor is compared with the approximately equidistant 64-PAM constellation which is the well known capacity maximizing high-SNR 1D constellation for the AWGN channel.

In the Nakagami-m channel with $m = 1$, which is the Rayleigh channel, the constellation optimized for $m = 1$ shows a 0.4 dB gain in comparison to 64-PAM at a BLER of 10^{-4}. For the case of $m = 3$, the constellation optimized for $m = 3$ shows a 0.2 dB gain in comparison to equidistant 64-PAM at a BLER of 10^{-4}, and for the case $m \to \infty$, which is the AWGN channel, the constellation optimized for $m = 10$ performs approximately the same as 64-PAM.

Fig. 5 shows the comparison of the BLER of 2D and 4D constellations in the AWGN channel for 4 bpcu. The length of the block is considered to be two channel uses since the size of the largest constellation is 4D in these figures. These results indicate that the 16-2D constellations, optimized either by solving problem (23) by setting $m = 10$ or by solving problem (29), perform similarly to each other and have approximately the same performance as the 16-2D constellation optimized in [3] or a 16-HEX constellation. Furthermore, all these 16-2D optimized constellations work 0.4 to 0.5 dB better than 16-QAM. The 256-4D constellation optimized in [3] performs around 0.2 dB better
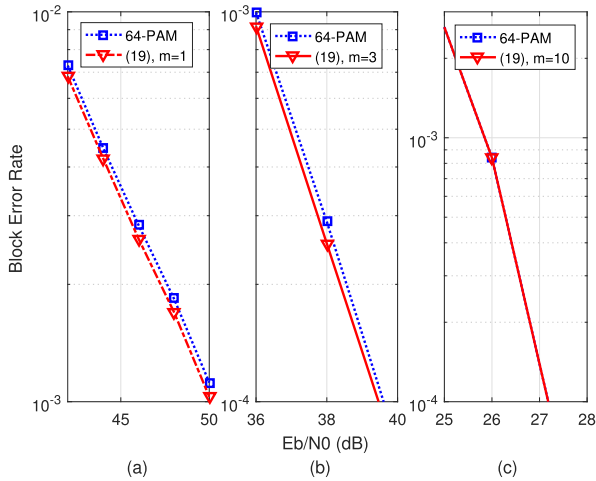
FIGURE 4. BLER comparison of a 1D constellation with a SISO configuration for 6 bpcu in Nakagami-*m* channels with different values of *m*, a) equidistant 64-PAM vs. 64-PAM optimized for *m* = 1 in Nakagami-*m* fading with *m* = 1, b) equidistant 64-PAM vs. 64-PAM optimized for *m* = 3 in Nakagami-*m* fading with *m* = 3 , c) equidistant 64-PAM vs. 64-PAM optimized for *m* = 10 in an AWGN channel.
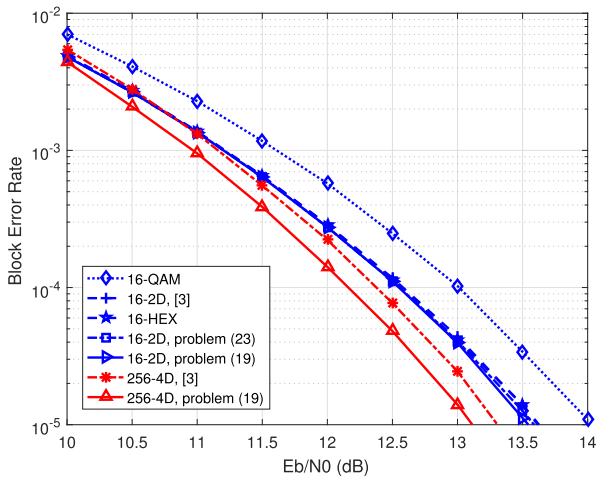

FIGURE 5. BLER comparison of a 2D constellation with a SISO configuration for 4 bpcu in an AWGN channel.

than optimized 16-2D constellations, while the 256-4D constellation optimized by solving problem (23) with $m = 10$ shows an additional 0.2 dB gain. Moreover, the performance of some of these constellations were checked in the Rayleigh channel and, as expected, the 16-2D constellation designed for Rayleigh outperforms the 2D constellation optimized for AWGN by 0.2 dB, and the 16-QAM constellation by 0.4 dB at a BLER of 10^{-5}.

Constellations optimized for minimizing the BER can be achieved by solving problem (23) on the SER and finding the best bit-to-symbol mapping by using the binary switching algorithm as described in Section IV, which we refer to as method A, or alternatively by solving problem (24) on the BER which is the joint optimization of the constellation shape and the bit-to-symbol mapping, which we refer to as method B. Here, we compare these two methods. Fig. 6 illustrates the BER comparison of different 16-2D
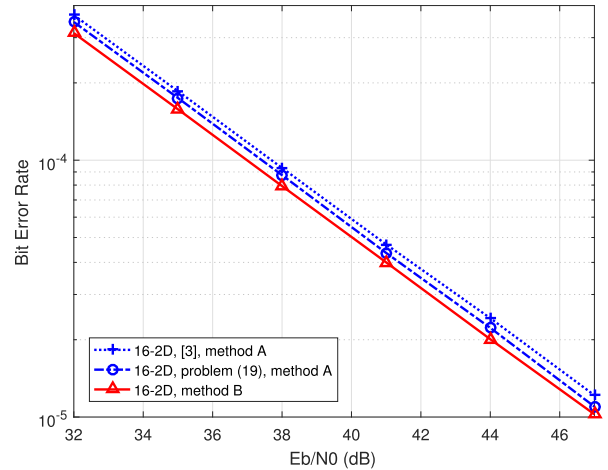
constellations in the SISO Rayleigh channel. It shows that the 16-2D constellation constructed based on method A by solving the problem (23) with $m = 1$ outperforms the 16-2D constellation constructed based on method A by using the constellation optimized in [3] for 0.4 dB at a BLER of 10^{-5}; the 16-2D constellation optimized based on method B with $m = 1$ provides an additional 0.4 dB gain.

For the case of the AWGN channel where we used a constellation optimized for the AWGN channel, there is only a small preference in performance for the constellation optimized using method B in comparison to method A, since as we observe in Fig. 2(a) and Fig. 2(b), constellations optimized for SER using bound (17) and for BER using bound (22) already have quite similar HEX-like shapes.
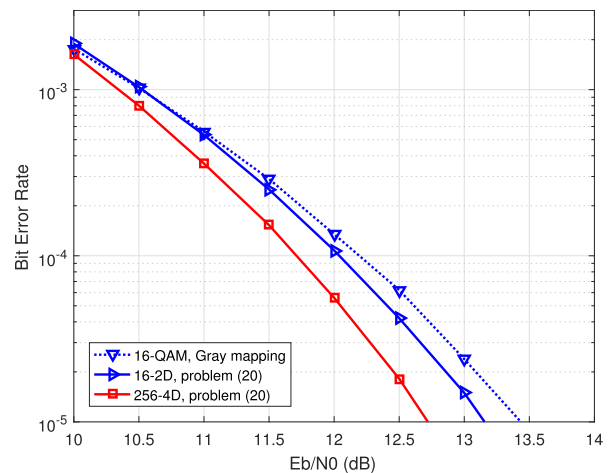

FIGURE 6. BER comparison of 2D constellations with a SISO configuration for 4 bpcu in a Rayleigh channel.

FIGURE 7. BER comparison of 2D constellation with a SISO configuration for 4 bpcu in an AWGN channel.

In Fig. 7, the BER performance of the 2D constellation optimized by solving problem (24) under a SISO antenna configuration and in the AWGN channel is examined. Among 2D constellations, 16-QAM with Gray mapping

is outperformed by the 16-2D constellation optimized for Nakagami-m with $m = 10$ by 0.3 dB at a BLER of 10^{-5}. Furthermore, the 256-4D constellation optimized for Nakagami-m with $m = 10$ outperforms the optimized 16-2D constellation by 0.5 dB at a BLER of 10^{-5}.

The above results show that by increasing the dimensionality of the constellation, there is more space for points to be further apart and this improves performance. Furthermore, by increasing the number of points of a constellation the performance gap between constellations optimized based on the bounds (17) and (22) and distance based constellations (e.g. [3]) increases. Results of this section are summarised in Table. 1.

TABLE 1. Performance advantage of optimized constellations in comparison with the best-known constellations in the literature for the SISO system.

Constellation	m	bpcu	Metric	Performance Advantage
64-1D	1	6	BLER	0.4 dB
64-1D	3	6	BLER	0.2 dB
64-1D	10	6	BLER	0 dB
16-2D	10	4	BLER	~ 0 dB
256-4D	10	4	BLER	0.2 dB
16-2D	10	4	BER	0.4 dB
256-4D	10	4	BER	0.8 dB

B. RESULTS FOR THE MIMO CONFIGURATION

In this part of the performance evaluation, as the baseline, OSTBCs with QAM constellations are compared against the schemes $\mathbf{G}_1$-$\mathbf{G}_3$, which consists of the use of multidimensional constellations with OSTBC. Since BLER (or the BER of a block) is used in the comparisons, constellations were optimized by using the problems (23) and (24), and; therefore, one multidimensional constellation is used in each space-time code block. As a reference for comparison, the same scheme is constructed by using OSTBC and the constellation proposed in [3]. The scheme is also compared with the Golden code [26] and the algebraic MISO code in [32] which we refer to as the "Oggier code". The constellations used with the Golden code for 2 bpcu and 4 bpcu are BPSK and QPSK, respectively, and with the Oggier code for 1 bpcu is BPSK. Furthermore, the scheme is compared with the QOSTBC with optimal rotation in [35], used with QPSK for a spectral efficiency of 2 bpcu.

In Fig. 8 the BLER performance of the Golden code, Alamouti's OSTBC $\mathbf{G}_0$ and the scheme $\mathbf{G}_1$, all with 2 bpcu, are compared in a Rayleigh channel. This result shows that scheme $\mathbf{G}_1$ with a constellation optimized by solving the problem (23) has the same performance as scheme $\mathbf{G}_1$ with a constellation optimized in [3]. Both schemes outperform OSTBC by 0.4 dB in a 2×1 configuration and by 0.5 dB in a 2×2 configuration at a BLER of 10^{-4}. Furthermore, the Golden code in a 2×2 configuration shows a BLER worse than OSTBC. Indeed, most algebraic codes are designed for high rates and therefore show poor performance at low rates since not all their degrees of freedom are well exploited.
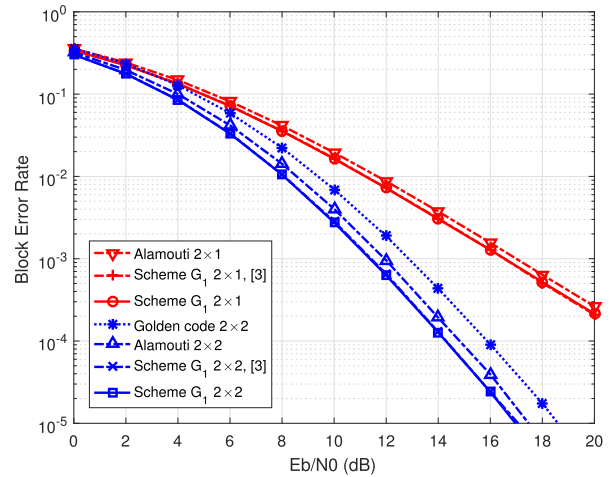

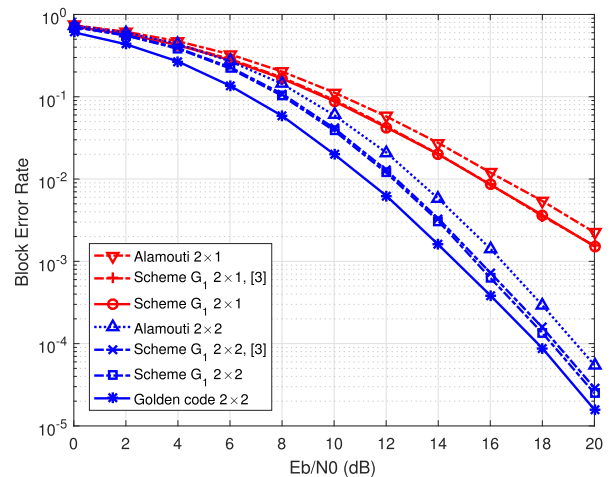**FIGURE 8.** BLER comparison of scheme $\mathbf{G}_1$, OSTBC and the Golden code for 2 bpcu.

FIGURE 9. BLER comparison of the scheme $\mathbf{G}_1$, OSTBC and the Golden code for 4 bpcu.

Fig. 9 shows the performance comparison of scheme $\mathbf{G}_1$ with OSTBC in 2×1 and 2×2 configurations and the Golden code 2×2 for 4 bpcu in a Rayleigh channel. The outcome indicates that the scheme $\mathbf{G}_1$ with a constellation optimized by solving the problem (23) and with a constellation optimized in [3] perform the same. They also work better than OSTBC as one of the best codes for the 2×1 configuration, by 0.9 dB at a BLER of 10^{-3}. Furthermore, for the 2×2 antenna configuration, it is 0.9 dB better than OSTBC and only 0.5 dB worse than the Golden code at 10^{-4}. Note that the Golden code 2×2 outperforms $\mathbf{G}_1$ since it benefits from more degrees of freedom, but it also has four times more complexity in terms of complex multiplications in each search for ML decoding even though the number of searches is the same as that in the scheme.

Fig. 10 shows the error performance of the schemes $\mathbf{G}_2$ and $\mathbf{G}_3$ for 3×1 and 4×1 antenna configurations, respectively, in a Rayleigh channel. The schemes $\mathbf{G}_2$ and $\mathbf{G}_3$
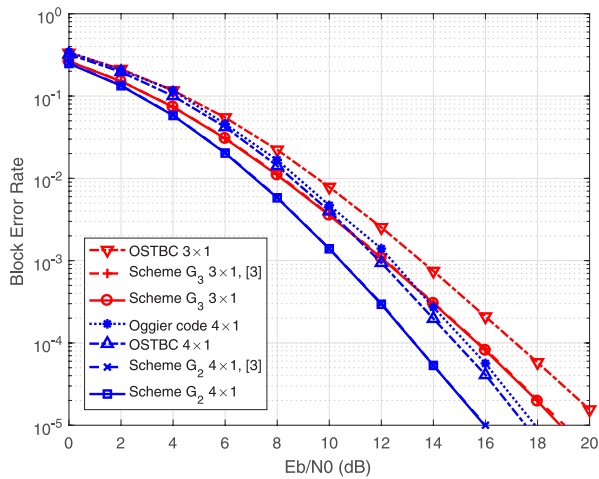
FIGURE 10. BLER comparison of the schemes G_2 and G_3, OSTBC and the Oggier code for 1 bpcu, with $N_r = 1$.

FIGURE 12. BLER comparison of the scheme G_2, OSTBC and QOSTBC for 2 bpcu.

have approximately the same performance when used with either the constellation optimized by solving the problem (23) or the constellation optimized in [3], and they outperform OSTBC by 1.5 dB in 3×1 and in 4×1 configurations at a BLER of 10^{-4}. Furthermore, the BLER comparison of the scheme and OSTBC in 3×2 and 4×2 configurations in Fig. 11 shows 1.7 dB and 1.8 dB improvement at 10^{-4}, respectively. To compare the scheme with algebraic codes, the recently designed MISO code in [32] (the "Oggier code") that can support lower rates was tested; similar to the Golden code in Fig. 8, its BLER is worse than the corresponding OSTBC.
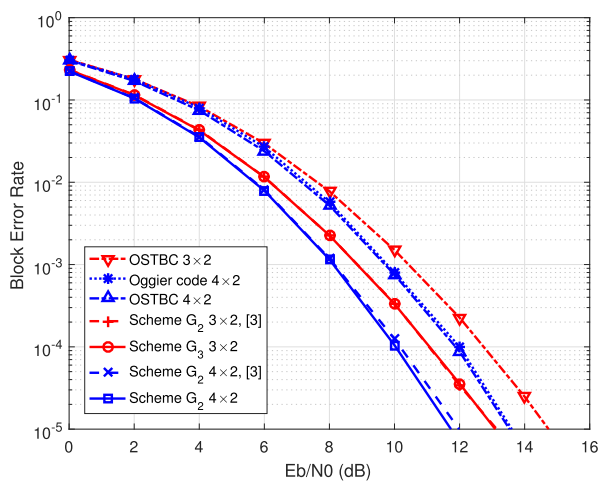
achieved at the expense of more decoding complexity. In the case of QOSTBC, joint pairwise decoding results in a lower number of searches, but each search is more complex than the decoding of the scheme. Furthermore, unlike the previous figures, the performance of the scheme with the constellation achieved from solving the problem (23) outperforms the scheme with a constellation optimized in [3] by 0.3 dB and 0.2 dB for 4×1 and 4×2 configurations, respectively. In comparison to [3], since the modulation is optimized for the Rayleigh fading channel, the performance is improved.

FIGURE 11. BLER comparison of the schemes G_2 and G_3, OSTBC and the Oggier code for 1 bpcu, with $N_r = 2$.

FIGURE 13. BER comparison of the scheme G_2 and QOSTBC for 2 bpcu.

Fig. 12 shows the performance of the scheme G_2 in comparison to OSTBC and QOSTBC 4×1 and 4×2 for 2 bpcu. The results show that the scheme outperforms OSTBC by around 4 dB at 10^{-3} and also outperforms QOSTBC 4×1 and 4×2 by 0.8 dB and 0.4 dB at 10^{-4}, respectively. Note that the improvement in comparison to OSTBC or QOSTBC is
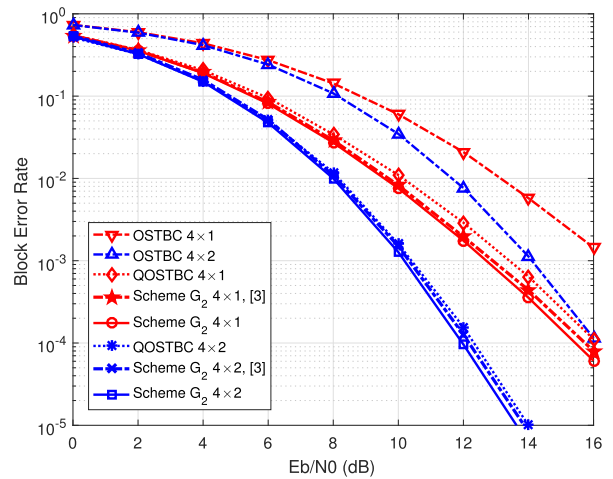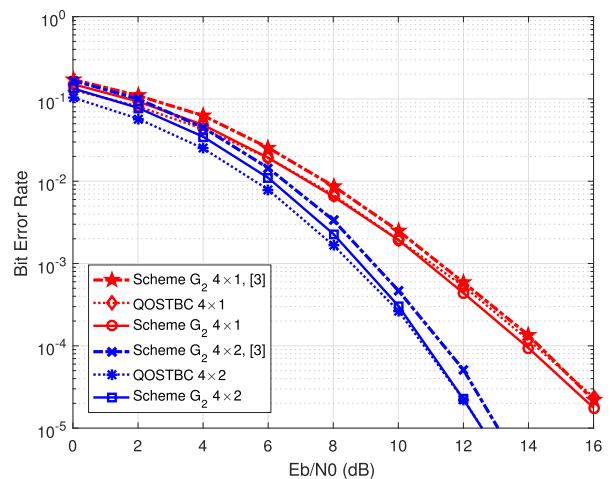
The BER of the scheme G_2 in comparison to the QOSTBC for 4×1 and 4×2 configurations is shown in Fig. 13. For a 4×1 configuration, scheme G_2 with a constellation optimized by solving the problem (23) outperforms scheme G_2 with method A and a constellation optimized in [3]. It also outperforms QOSTBC by 0.3 dB at BER of 10^{-5}. For a 4×2 configuration, the scheme G_2 with a constellation optimized by solving the problem (23) and QOSTBC perform
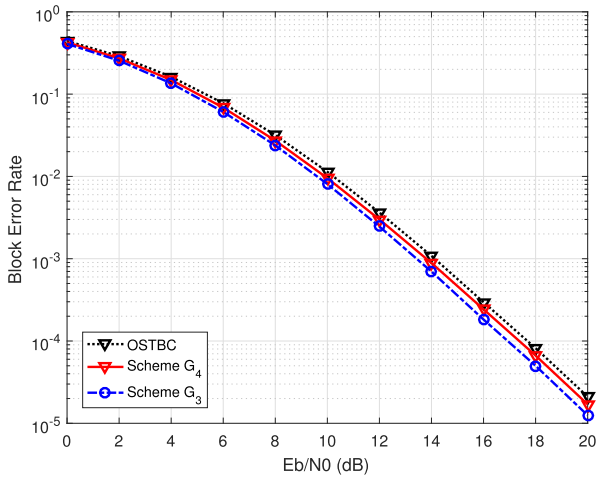
FIGURE 14. BLER comparison of the generalized scheme and OSTBC in three different values of σ^2 for 1.5 bpcu.

TABLE 2. Performance advantage of optimized constellations in comparison with the best-known constellations in the literature for the MIMO Rayleigh fading channel and 2 bpcu.

Scheme	Constellation	Metric	Performance Advantage
$\mathbf{G}_1$, 2×1	16-4D	BLER	0 dB
$\mathbf{G}_1$, 2×2	16-4D	BLER	0 dB
$\mathbf{G}_2$, 4×1	256-6D	BLER	0.3 dB
$\mathbf{G}_2$, 4×2	256-6D	BLER	0.2 dB
$\mathbf{G}_2$, 4×1	256-6D	BER	0.5 dB
$\mathbf{G}_2$, 4×2	256-6D	BER	0 dB

approximately the same and outperform scheme $\mathbf{G}_2$ with method A and a constellation optimized in [3] by 0.5 dB at BER of 10^{-5}.

Finally, Fig. 14 shows the performance of the generalized scheme $\mathbf{G}_4$ with one 16-4D constellation and a QPSK constellation in comparison with the scheme $\mathbf{G}_3$ for a 3×1 antenna configuration used with a 64-6D constellation and an OSTBC with a QPSK constellation in a Rayleigh channel. For the case of $\sigma^2 = 0$, the scheme $\mathbf{G}_3$ outperforms $\mathbf{G}_4$ by 0.4 dB and $\mathbf{G}_4$ outperforms OSTBC by 0.3 dB at the BLER of 10^{-4}. As explained in Section II, the difference of the generalized scheme $\mathbf{G}_4$ and scheme $\mathbf{G}_3$ can be explained by using a complexity-performance trade-off. For the ML decoding of scheme $\mathbf{G}_3$, 64 searches in 6D space are necessary while for the generalized scheme $\mathbf{G}_4$, only 16 searches in 4D space and 4 searches in 2D space are necessary. Thus, the generalized scheme has a lower decoding complexity and since the points have less space to be far apart, the performance is degraded. Furthermore, similar to the results in Fig. 15, if the channel is estimated imperfectly, the BLER shows an error floor.

By designing multidimensional constellations adapted to OSTBC, high performance improvements can be achieved at the expense of increasing the complexity of decoding. Increasing the dimensionality of the constellation improves the performance even though the size of the employed OSTBC, including the number of antennas and the number of time slots, may be increased. Indeed, this is the main reason that schemes $\mathbf{G}_2$ and $\mathbf{G}_3$ provide more gain in comparison to $\mathbf{G}_1$. Additionally, as observed in the results of the generalized scheme shown in Fig. 14, there exists a complexity-performance trade-off when part of the independent symbols of the OSTBC are used to carry dependent dimensions of multidimensional constellations. Performance advantages of the results of this section are summarized in Table. 2 for 2 bpcu. Note that for 1 bpcu, the gain in comparison to the best-known constellations is

approximately zero. For reference, the performance of the scheme under imperfect channel estimation has been reported in Appendix C.

When the regular constellations such as QAM constellations are used, the decision regions are very regular. Therefore, designing a low complexity ML decoder for these constellations is possible using the simple decision thresholds. However, for the irregular constellations, the decision regions are very complex and designing a decoder based on these regions may be infeasible. In both cases, sphere decoders may decrease the decoding complexity [20]. However, for regular constellations, sphere decoders with lower complexity can be designed.

VI. CONCLUSIONS

In this paper, two bounds on the performance of the SER and BER of multidimensional constellations in a Nakagami-m fading channel at high SNR are derived. These bounds are used to obtain the constellations that minimize the SER and BER. The convexity of the SER and BER upper bounds is proven for 1D constellations. As the result of optimization, SER-minimizing 1D, 2D and multidimensional constellations overcome the best-known constellations in SISO configuration. The BER-minimizing constellations optimized using the BER bound outperform the constellations found based on the independent optimization of shape and the bit-to-symbol mapping. In addition, it is shown that adapting the constellations based on the channel parameter m can improve the performance.

The multidimensional constellations were also optimized for the OSTBC and it is observed that these constellations can improve the BLER of the OSTBC in comparison to regular 2D QAM constellations. The OSTBC with multidimensional constellations works well for low-to-moderate spectral efficiencies where all degrees of freedom of algebraic codes cannot be fully exploited. Even though the non-orthogonal algebraic codes may provide better performance than orthogonal STBCs at high spectral efficiencies, the optimized constellations provide a trade-off between decoding complexity and performance. Furthermore, the scheme outperforms QOSTBCs but this improvement is achieved at the expense of higher ML decoding complexity. Finally, the proposed generalized scheme can provide a complexity-performance trade-off for OSTBCs with multidimensional constellations.

APPENDIX A

A.1 Derivation of (14): SER Union Bound for a Nakagami-m Channel

By using the Chernoff bound, (13) is upper bounded as

$$
\begin{aligned}
&P(\mathbf{s} \rightarrow \hat{\mathbf{s}} \mid \mathbf{H}) \\
&\leq \exp\left(-\left(\frac{\sum_{j=1}^{N_r}\sum_{i=1}^{N_t}\alpha_{ij}^2}{4N_0}\right)\sum_{k=1}^{K}\left|s^{(k)}-\hat{s}^{(k)}\right|^2\right) \\
&= \prod_{j=1}^{N_r}\prod_{i=1}^{N_t}\exp\left(-\left(\frac{\alpha_{ij}^2}{4N_0}\right)\sum_{k=1}^{K}\left|s^{(k)}-\hat{s}^{(k)}\right|^2\right).
\end{aligned} \tag{30}
$$

By considering the distribution of α_{ij}^2 for Nakagami-m fading, the PEP can be upper bounded further as

$$
P(\mathbf{s} \rightarrow \hat{\mathbf{s}}) \leq \frac{4^{mN_tN_r}}{\prod_{j=1}^{N_r}\prod_{i=1}^{N_t}\left(\bar{\gamma}_{ij}\frac{\sum_{k=1}^{K}|s^{(k)}-\hat{s}^{(k)}|^2}{m}+4\right)^m}. \tag{31}
$$

From (31), a union bound on the SER of OSTBC with multidimensional constellations can be derived as (14).

A.2 Derivation of (17): The Second SER Union Bound for a Nakagami-m Channel

At high SNR where $\bar{\gamma}_{ij}/m \gg 4$, the PEP in (31) can in turn be bounded by

$$
P(\mathbf{s} \rightarrow \hat{\mathbf{s}}) \leq \frac{(4m)^{mN_tN_r}}{\left(\prod_{j=1}^{N_r}\prod_{i=1}^{N_t}\bar{\gamma}_{ij}\right)\left(\sum_{k=1}^{K}\left|s^{(k)}-\hat{s}^{(k)}\right|^2\right)^{mN_tN_r}}. \tag{32}
$$

From (32), the corresponding union bound on the SER can be derived as (17).

A.3 Derivation of (21): SER Union Bound for an AWGN Channel

To prove (21), starting from (30) and by considering $\alpha_{ij}^2 = 1$ for the AWGN channel, the PEP upper bound is written as

$$
P(\mathbf{s} \rightarrow \hat{\mathbf{s}}) \leq \exp\left(-\left(\frac{N_rN_t}{4N_0}\right)\sum_{k=1}^{K}\left|s^{(k)}-\hat{s}^{(k)}\right|^2\right). \tag{33}
$$

Finally, by considering the union bound, (21) can be derived.

VII. APPENDIX B

B.1 Proof of Convexity of (14) for 1D Constellations

For simplicity let us assume $\bar{\gamma}_{ij}$ is the same for all paths, i.e., $\bar{\gamma}' = \bar{\gamma}_{ij}$. For 1D constellations, (31) can be written as

$$
P(\mathbf{s} \rightarrow \hat{\mathbf{s}}) \leq \frac{C''}{\left(\frac{\bar{\gamma}'}{m}(s-\hat{s})^2+4\right)^{mN_tN_r}}, \tag{34}
$$

where $C'' = 4^{mN_tN_r}$. Setting $\delta = (s-\hat{s})$ and $y = C''(\frac{\bar{\gamma}'}{m}\delta^2 + 4)^{-mN_tN_r}$, we take the second derivative of y to examine the

convexity. It can be given as

$$
\frac{d^2y}{d\delta^2} = 2\bar{\gamma}'N_tN_rC''\frac{(2mN_tN_r+1)\delta^2\bar{\gamma}'/m-4}{(\frac{\bar{\gamma}'}{m}\delta^2+4)^{2+mN_tN_r}}. \tag{35}
$$

For convexity of (31), $d^2y/d\delta^2$ should be positive. This only happens if the following condition is satisfied:

$$
x := \frac{2}{\sqrt{\frac{\bar{\gamma}'}{m}(2mN_tN_r+1)}} < |\delta|. \tag{36}
$$

Therefore, the minimum distance of the constellation points should be greater than x. For OSTBCs, the total average SNR of each received matrix $\mathbf{G}$ is simplified as $\bar{\gamma} = E[\sum_i\sum_j\alpha_{ij}^2]/N_0 = N_tN_r/N_0$, which results in $\bar{\gamma} = N_tN_r\bar{\gamma}'$. Therefore, x can be rewritten in terms of the total average SNR as (16). Given the convexity condition in (36), the upper bound on the PEP in (34) is convex on mutually excluded sets since either $\delta > x$ or $\delta < -x$ for each pair of points. Because the sum of convex functions preserves the convexity [37], the union bound on the PEP in (17) is also convex in the convexity regions of (34) given in (15). The more general case, where $\bar{\gamma}_{ij}$ is different for each path, can be proven by considering the log-convexity of (31) for 1D constellations.

B.2 Proof of Convexity of (17) for 1D Constellations

For 1D constellations, (32) can be written as

$$
P(\mathbf{s} \rightarrow \hat{\mathbf{s}}) \leq \frac{C''}{(s-\hat{s})^{2mN_tN_r}}, \tag{37}
$$

where $C'' = (4m)^{mN_tN_r}/\bar{\gamma}$. We set $y = C''(s-\hat{s})^{-2mN_tN_r}$. Hence $d^2y/d\delta^2$ can be given as

$$
\frac{d^2y}{d\delta^2} = 2mN_tN_rC''(2mN_tN_r+1)\delta^{-2(mN_tN_r+1)}. \tag{38}
$$

For convexity of (38), it is sufficient that $\delta > 0$. First, we explain why δ can be non-negative. Without loss of generality, we can assume a specific ordering for 1D constellations, since symbol labelling is not effective on the SER. Thus, we can set $s_1 \leq s_2 \leq \ldots \leq s_{2^d}$. Therefore, we can assume δ is always non-negative so the convexity condition is limited to $\delta \neq 0$. This observation is consistent with the asymptotic behavior of (16) since, as $\bar{\gamma}$ tends to infinity, x tends to zero. Therefore, PEP in (37) is a convex function on mutually excluded sets corresponding to $\delta > 0$ or $\delta < 0$. The rest of the proof is the same as the last part in Appendix B.1.

APPENDIX C
PERFORMANCE OF THE CONSTELLATIONS UNDER IMPERFECT CHANNEL ESTIMATION

The performance of $\mathbf{G}_3$ for a 3×1 antenna configuration under imperfect channel estimation in a Rayleigh fading channel is evaluated in Fig. 15. The channel estimation method is assumed to be linear minimum mean square error (LMMSE). As described in [52] and [53], the variance of the channel estimation error with LMMSE can be modelled with a factor σ^2 ranging from zero to one that corresponds to
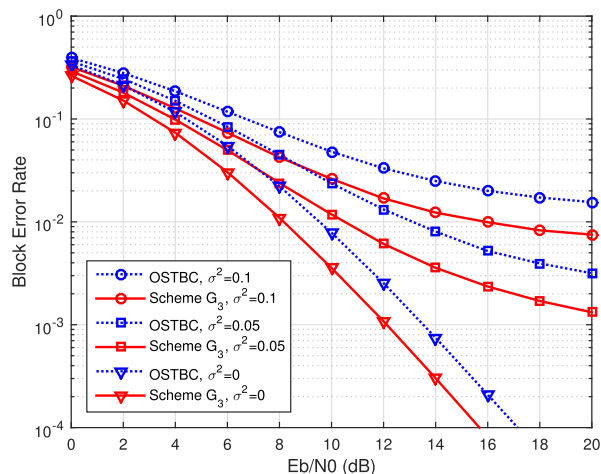
FIGURE 15. BLER comparison of the scheme G_3 in three different values of σ^2 for 2 bpcu with a 3×1 antenna configuration.

a coherent receiver (perfect channel estimation) when it is set to zero and a non-coherent receiver (no channel estimation) when it is set to one. It can be seen that when the channel is estimated imperfectly, the BLER curves show an error floor at relatively high values.

ACKNOWLEDGMENT

REFERENCES

[1] J. H. Conway, and N. J. A. Sloane, *Sphere Packings, Lattices and Groups*, 3rd edition, New York, NY, USA: Springer-Verlag, 1999.

[2] N. J. A. Sloane, R. H. Hardin, T. S. Duff, and J. H. Conway, "Minimal-energy clusters of hard spheres," Discrete and Computational Geom., vol. 14, no. 1, pp. 237-259, Oct. 1995.

[3] M. Beko and R. Dinis, "Designing good multi-dimensional constellations," *IEEE Wirel. Commun. Letters*, vol. 1, no. 3, pp. 221-224, Apr. 2012.

[4] A. Bin Sediq, P. Djukic, H. Yanikomeroglu, and J. Zhang, "Optimized nonuniform constellation rearrangement for cooperative relaying," *IEEE Trans. Veh. Technol.*, vol. 60, no. 5, pp. 2340-2347, June 2011.

[5] H. Khoshnevis, I. Marsland, and H. Yanikomeroglu, "Irregular multidimensional constellations for orthogonal STBCs," in *Proc. IEEE Globecom*, San Diego, CA, USA, Dec. 2015.

[6] A. Yadav, M. Juntti, and J. Lilleberg, "Partially coherent constellation design and bit-mapping with coding for correlated fading channels," *IEEE Trans. Commun.*, vol. 61, no. 10, pp. 4243-4255, Oct. 2013.

[7] G. Caire, G. Taricco, and E. Biglieri, "Bit-interleaved coded modulation," *IEEE Trans. Inform. Theory*, vol. 44, no. 3, pp. 927-945, May 1998.

[8] A. Chindapol and J. A. Ritcey, "Design, analysis and performance evaluation for BICM-ID with square QAM constellations in Rayleigh fading channels," *IEEE J. Sel. Areas Commun.*, vol. 19, no. 5, pp. 944-957, May 2001.

[9] A. Gersho and V. Lawrence, "Multidimensional signal constellations for voiceband data transmission," *IEEE J. Sel. Areas Commun.*, vol. 2, no. 5, pp. 687-702, Sept. 1984.

[10] G. D. Forney, and L-F. Wei, "Multidimensional constellations - Part I: introduction, figures of merit, and generalized cross constellations," *IEEE J. Sel. Areas Commun.*, vol. 7, no. 6, pp. 877-892, Aug. 1989.

[11] G. D. Forney, "Multidimensional constellations - Part II: Voronoi constellations," *IEEE Trans. Inf. Theory*, vol. 7, no. 6, pp. 941-958, Aug. 1989.

[12] J. E. Porath and T. Aulin, "Design of multidimensional signal constellations," *IEE Proc. Commun.*, vol. 150, no. 5, pp. 317-323, Oct. 2003.

[13] V. Tarokh, H. Jafarkhani, and A. R. Calderbank, "Space-time block codes from orthogonal designs," *IEEE Trans. Inf. Theory*, vol. 45, no. 5, pp. 1456-1467, July 1999.

[14] S. Alamouti, "A simple transmit diversity technique for wireless communications," *IEEE J. Sel. Areas Commun.*, vol. 16, no. 8, pp. 1451-1458, Oct. 1998.

[15] *LTE; Evolved Universal Terrestrial Radio Access (E-UTRA); Physical channels and modulation*, 3GPP TS 36.211 version 12.4.0 release 12, Feb. 2015.

[16] H. Jafarkhani, "A quasi-orthogonal space-time block code," *IEEE Trans. Commun.*, vol. 49, no. 1, pp. 1-4, Jan. 2001.

[17] N. Sharma and B. Papadias, "Improved quasi-orthogonal codes through constellation rotation," in *Proc. IEEE Int. Conf. on Acoust., Speech, and Signal Process.*, Orlando, FL, USA, May 2002.

[18] W. Su and X-G. Xia, "Signal constellations for quasi-orthogonal space-time block codes with full diversity," *IEEE Trans. Inf. Theory*, vol. 50, no. 10, pp. 2331-2347, Oct. 2004.

[19] H. Yao and G. W. Wornell, "Achieving the full MIMO diversity-multiplexing frontier with rotation-based space-time codes," in *Proc. Allerton Conf. Commun., Control, and Computing*, Monticello, VA, USA, Oct. 2003.

[20] M. O. Damen, A. Tewfik, and J-C. Belfiore, "A construction of a space-time code based on number theory," *IEEE Trans. Inf. Theory*, vol. 48, no. 3, pp. 753-760, Mar. 2002.

[21] A. Scaglione, P. Stoica, S. Barbarossa, G. B. Giannakis, and H. Sampath, "Optimal designs for space-time linear precoders and decoders," *IEEE Trans. Signal Process.*, vol. 50, no. 5, pp. 1051-1064, May 2002.

[22] H. El Gamal and M. O. Damen, "Universal space-time coding," *IEEE Trans. Inf. Theory*, vol. 49, pp. 1097-1119, May 2003.

[23] M. O. Damen, H. El Gamal and N. C. Beaulieu, "Linear threaded algebraic space-time constellations," *IEEE Trans. Inf. Theory*, vol. 49, no. 10, pp. 2372-2388, Oct. 2003.

[24] B. A. Sethuraman, B. S. Rajan, and V. Shashidhar, "Full-diversity, high-rate space-time block codes from division algebras," *IEEE Trans. Inf. Theory*, vol. 49, no. 10, pp. 2596-2616, Oct. 2003.

[25] P. Dayal and M. K. Varanasi, "An optimal two transmit antenna space-time code and its stacked extensions," *IEEE Trans. Inf. Theory*, vol. 51, no. 12, pp. 4348-4355, Dec. 2005.

[26] J-C. Belfiore, G. Rekaya, and E. Viterbo, "The golden code: A 2×2 full-rate space-time code with nonvanishing determinants," *IEEE Trans. Inf. Theory*, vol. 51, no. 4, pp. 1432-1436, Apr. 2005.

[27] F. Oggier, G. Rekaya, J-C. Belfiore, and E. Viterbo, "Perfect space-time block codes," *IEEE Trans. Inf. Theory*, vol. 52, no. 9, pp. 3885-3902, Sept. 2006.

[28] M. Janani and A. Nosratinia, "Efficient space-time block codes derived from quasi-orthogonal structures," *IEEE Trans. Wireless Commun.*, vol. 6, pp. 1643-1646, May 2007.

[29] S. Sezginer and H. Sari, "Full-rate full-diversity 2×2 space-time codes of reduced decoder complexity," *IEEE Commun. Lett.*, vol. 11, no. 12, pp. 973-975, Dec. 2007.

[30] S. Sezginer, H. Sari and E. Biglieri, "On high-rate full-diversity 2×2 space-time codes with low-complexity optimum detection," *IEEE Trans. Commun.*, vol. 57, no. 5, pp. 1532-1541, May 2009.

[31] L. Hanzo, O. R. Alamri, M. El-Hajjar, and N. Wu, *Near-Capacity Multi-Functional MIMO Systems*, New York, NY, USA: Wiley, 2009.

[32] F. Oggier, C. Hollanti, and R. Vehkalahti, "An algebraic MIDO-MISO code construction," in *Proc. 8th Int. Conf. on Signal Process. and Commun.*, Bangalore, India, July 2010.

[33] V. Tarokh, N. Seshadri, and A. R. Calderbank, "Space-time codes for high data rate wireless communication: performance criterion and code construction," *IEEE Trans. Inf. Theory*, vol. 44, no. 2, pp. 744-765, Mar. 1998.

[34] D. M. Ionescu, "New results on space-time code design criteria," *IEEE WCNC*, New Orleans, LA, USA, Sept. 1999,.

[35] H. Jafarkhani, *Space-Time Coding: Theory and Practice*, Cambridge, UK: Cambridge Univ. Press, 2005.

[36] A. Dogandžic, "Chernoff bounds on pairwise error probabilities of space-time codes," *IEEE Trans. Inf. Theory*, vol. 49, no. 5, pp. 1327-1336, May 2003.

[37] S. Boyd and L. Vandenberghe, *Convex Optimization*, Cambridge, UK: Cambridge Univ. Press, 2004.

[38] J. Proakis and M. Salehi, *Digital Communications*, 5th ed., New York, NY, USA: McGraw-Hill, 2007.

[39] R. J. Vanderbei and D. F. Shanno, "An Interior-Point Method for Nonconvex Nonlinear Programming," *Computational Optimization and Applicat.*, vol.13, no. 1-3, pp. 231-252, Apr. 1999

[40] J. Nocedal and S. J. Wright, *Numerical Optimization*, New York, NY, USA: Springer-Verlag, 2006.

[41] F. Kayhan and G. Montorsi, "Constellation design for memoryless phase noise channels," *IEEE Trans. Wireless Commun.*, vol. 15, no. 5, pp. 2874-2883, May 2014.

[42] K. Zeger and A. Gersho, "Pseudo-Gray coding," *IEEE Trans. Commun.*, vol. 38, no. 12, pp. 2147-2158, Dec. 1990.

[43] F. Schreckenbach, N. Gortz, J. Hagenauer, and G. Bauch, "Optimization of symbol mappings for bit-interleaved coded modulation with iterative decoding," *IEEE Commun. Lett.*, vol. 7, no. 12, pp. 593-595, Dec. 2003.

[44] M. F. Barsoum, C. Jones, and M. Fitz, "Constellation design via capacity maximization," in *Proc. IEEE ISIT*, pp. 1821-1825, Nice, France, June 2007.

[45] Y. Li and X-G. Xia, "Constellation mapping for space-time matrix modulation with iterative demodulation/decoding," *IEEE Trans. Commun.*, vol. 53, no. 5, pp. 764-768, May 2005.

[46] J. H. Conway and N. J. A. Sloane, "A fast encoding method for lattice codes and quantizers," *IEEE Trans. Inf. Theory*, vol. 26, no. 6, pp. 820-824, Nov. 1983.

[47] G. J. Foschini, R. D. Gitlin, and S. B. Weinstein, "Optimization of two-dimensional signal constellations in the presence of Gaussian noise," *IEEE Trans. Commun.*, vol. 22, no. 1, pp. 28-38, Jan. 1974.

[48] G. D. Forney, Jr, R. G. Gallager, G. R. Lang, F. M. Longstaff, and S. U. Qureshi, "Efficient modulation for band-limited channels," *IEEE J. Sel. Areas Commun.*, vol. 2, no. 5, pp. 632-647, Sept. 1984.

[49] R. L. Graham and J. A. Sloane, "Penny-packing and two-dimensional codes," *Discrete and Computational Geom.*, vol. 5, no. 1, pp. 1-11, Jan. 1990.

[50] C. M. Thomas, M. Y. Weidner, and S. H. Durrani, "Digital amplitude-phase keying with M-ary alphabets," *IEEE Trans. Commun.*, vol. 22, no. 2, pp. 168-180, Feb. 1974.

[51] M. Kifle and M. Vanderaar, "Bounds and simulation results of 32-ary and 64-ary quadrature amplitude modulation for broadband-ISDN via satellite," NASA Technical Memorandum 106484, 1994.

[52] B. Hassibi and B. M. Hochwald, "How much training is needed in multipleâĂ"antenna wireless links?," *IEEE Trans. Inf. Theory*, vol. 49, no. 4, pp. 951-963, Apr. 2003.

[53] M. J. Borran, A. Sabharwal, and B. Aazhang, "Design criterion and construction methods for partially coherent multiple antenna constellations," *IEEE Trans. Wireless Commun.*, vol. 8, no. 8, pp. 4122-4133, Aug. 2009.

HOSSEIN KHOSHNEVIS (S'17) received the B.Sc. degree in electrical engineering from the University of Isfahan, Isfahan, Iran in 2009 and the M.Sc. degree in computer science from Saarland University, Saarbrücken, Germany in 2012. During his master's studies, he was a recipient of the International Max Planck Research School for Computer Science (IMPRS-CS) fellowship and he was with the Max Planck Institute for Informatics. He is currently working towards the Ph.D. degree at the Department of Systems and Computer Engineering, Carleton University, Ottawa, ON, Canada. During his studies towards Ph.D., he has been a member of the Huawei-Carleton collaborative research project.

His research interests include coding theory, digital communications and statistical signal processing.

IAN MARSLAND (M'98) received the B.Sc.Eng. (Hons.) degree in mathematics and engineering from Queen's University, Kingston, ON, Canada, in 1987, and the M.Sc. and Ph.D. degrees in electrical engineering from The University of British Columbia, Vancouver, BC, Canada, in 1994 and 1999, respectively.

From 1987 to 1990, he was with Myrias Research Corporation, Edmonton, AB, Canada, and CDP Communications Inc., Toronto, ON, where he was a Software Engineer. He is currently an Associate Professor with the Department of Systems and Computer Engineering, Carleton University, Ottawa, ON. His research interests fall in the area of wireless digital communication.

HALIM YANIKOMEROGLU (F'17) was born in Giresun, Turkey, in 1968. He received the B.Sc. degree in electrical and electronics engineering from the Middle East Technical University, Ankara, Turkey, in 1990, and the M.A.Sc. degree in electrical engineering (now ECE) and the Ph.D. degree in electrical and computer engineering from the University of Toronto, Canada, in 1992 and 1998, respectively.

From 1993 to 1994, he was with the Research and Development Group, Marconi Kominikasyon A.S., Ankara, Turkey. Since 1998, he has been with the Department of Systems and Computer Engineering, Carleton University, Ottawa, Canada, where he is currently a Full Professor. His research interests cover many aspects of wireless technologies with a special emphasis on cellular networks. In recent years, his research has been funded by Huawei, Telus, Allen Vanguard, Blackberry, Samsung, Communications Research Centre of Canada, and DragonWave. This collaborative research resulted in about 30 patents (granted and applied). He is a Distinguished Lecturer with the IEEE Communications Society and a Distinguished Speaker for the IEEE Vehicular Technology Society in 5G wireless technologies. He has been involved in the organization of the IEEE Wireless Communications and Networking Conference (WCNC) from its inception in 1998 in various capacities, including serving as a Steering Committee Member, an Executive Committee Member, and the Technical Program Chair or Co-Chair of WCNC 2004 (Atlanta), WCNC 2008 (Las Vegas), and WCNC 2014 (Istanbul). He was the General Co-Chair of the IEEE Vehicular Technology Conference (VTC2010-Fall) held in Ottawa and the General Chair of the IEEE VTC2017-Fall held in Toronto. He has served on the editorial boards of the IEEE Transactions on Communications, the IEEE Transactions on Wireless Communications, and the IEEE Communications Surveys and Tutorials. He was the Chair of the IEEE's Wireless Technical Committee.

He was with the TOBB University of Economics and Technology, Ankara, as a Visiting Professor, from 2011 to 2012. He is a registered Professional Engineer in the province of Ontario, Canada. He was a recipient of the IEEE Ottawa Section Outstanding Educator Award in 2014, the Carleton University Faculty Graduate Mentoring Award in 2010, the Carleton University Graduate Students Association Excellence Award in Graduate Teaching in 2010, and the Carleton University Research Achievement Award in 2009.

• • •